

Statistics of Lagrangian Trajectories in a Rotating Turbulent Flow

Priyanka Maity,* Rama Govindarajan,† and Samriddhi Sankar Ray‡

International Centre for Theoretical Sciences, Tata Institute of Fundamental Research, Hessaraghatta, Hobli, Bangalore - 560089, India

We investigate the Lagrangian statistics of three-dimensional rotating turbulent flows through direct numerical simulations. We find that the emergence of coherent vortical structures because of the Coriolis force leads to a suppression of the “flight-crash” events reported by Xu, *et al.* [Proc. Natl. Acad. Sci. (U.S.A) **111**, 7558 (2014)]. We perform systematic studies to trace the origins of this suppression in the emergent geometry of the flow and show why such a Lagrangian measure of irreversibility may fail in the presence of rotation.

The irreversibility of fully developed, homogeneous and isotropic turbulence, as well as the non-trivial spatio-temporal structure of its (Eulerian) velocity field shows up in an interesting way in the statistics of the kinetic energy along Lagrangian trajectories. Xu, *et al.* [1], measured the kinetic energy of a tracer along its trajectory, as a function of time, to show that the gain in kinetic energy (over time) is gradual whereas the loss is rapid. (The average energy, statistically, is of course constant over time.) This behaviour of the energy fluctuations is quantified most conveniently by the statistics of energy increments (gain or loss) at small, but fixed, time intervals. In the limiting case, the rate of change of the kinetic energy, or power, serves as a useful probe to understand how Eulerian irreversibility manifests itself in the Lagrangian framework. Bhatnagar, *et al.* [2], extended this idea to the case of heavy, inertial particles, preferentially sampling the flow, to disentangle the effects of irreversibility and flow geometry.

This feature of Lagrangian trajectories, dubbed as “flight-crash events” [1], is a consequence of the dissipative nature of turbulent flows as well as the spatial structure of the Eulerian field with its intense, though sparse, regions of vorticity and more abundant, though milder, regions of strain. However, so far, measurements have been confined only to flows which are statistically homogeneous and isotropic. Therefore it is natural to ask if *flight-crash* events are just as ubiquitous in turbulent settings with anisotropy and structures different from those seen in statistically homogeneous, isotropic turbulence. An obvious candidate for this is fully developed turbulent flows under rotation [3–5] which are seen in a variety of processes spanning scales ranging from the astrophysical [6–8], geophysical [9] to the industrial [10]. In all these phenomena, although the Coriolis force does no work, it leads to the formation of large-scale columnar vortices leading to dynamics quite different from non-rotating, three-dimensional flow. In particular, rotation gives rise to an enhanced accumulation of energy in modes perpendicular to the plane of rotation [11–13], an inverse energy cascade in 3D turbulence [14–16], generation of inertial waves [5, 17, 18], and an increase in length scales parallel to the axis of rotation [19]. Consequently, rotating turbulence has been the subject of much experimental [16–22] and theoretical [12–15, 23–28] investigations in the last few decades.

A striking effect of rotation is on the geometry of the flow. Rapid rotation leads to a two-dimensionalisation of the flow through the formation of columnar (cyclonic) vortices parallel to the rotation axis [3, 5, 29–31] as well as an emergent anisotropy through the breaking of the cyclone-anticyclone symmetry. This effect, characterised and measured in experiments [20–22, 32] and direct numerical simulations (DNS) [23, 24, 27], stems from an enhanced (cyclonic) vortex stretching because of the Coriolis force.

The effect of these emergent two-dimensional vortical structures in a three-dimensional flow on Lagrangian measurements has received attention only recently [31, 33–35]. In particular, Biferale, *et al.* [31], through state-of-the-art DNSs explored these consequences on the mixing and transport properties of particles (both tracers and inertial) in rotating turbulence. However, the effect of such coherent structures on individual Lagrangian (tracer) trajectories from the point of view of time-irreversibility remains an open one.

In this paper, we investigate this aspect of rotating turbulence and find that time-irreversibility, in the Lagrangian sense [1, 2], decreases as the effect of rotation, and hence columnar vortices, becomes stronger. These results are rationalised by careful measurements of the correlation between the topology of the flow and the tracer trajectories which suggests that the spatial structure of a flow is critical in determining the strength of *flight-crashes* even if the flow itself retains the same degree of irreversibility through a finite dissipation.

We begin with the three-dimensional Navier-Stokes equation

$$\frac{\partial \mathbf{u}}{\partial t} + (\mathbf{u} \cdot \nabla) \mathbf{u} + 2(\boldsymbol{\Omega} \times \mathbf{u}) = -\nabla P' + \nu \nabla^2 \mathbf{u} + \mathbf{f} \quad (1)$$

for the velocity field \mathbf{u} of a unit-density fluid rotating about a fixed axis with a rate $\boldsymbol{\Omega}$, along with the incompressibility condition $\nabla \cdot \mathbf{u} = 0$. We use an external forcing \mathbf{f} , on wavenumber(s) k_f , to drive the fluid (with kinematic viscosity ν) to a statistically steady state associated with an energy (viscous) dissipation rate ϵ . The pressure $P' = P_0 - \frac{1}{2}|\boldsymbol{\Omega} \times \mathbf{r}|^2$ absorbs the centrifugal contribution from the rotating frame along with the natural pressure P_0 in the fluid in absence of rotation.

Apart from the Reynolds number, rotational turbulent flows in a box of size L (in our case, $L = 2\pi$), with typical room-mean-square velocities u_{rms} , are conveniently characterized by a second dimensionless number, the Rossby number $Ro \equiv u_{\text{rms}}/(2L\Omega)$, which is the ratio of the inertial to the Coriolis term. Furthermore, the additional Coriolis term leads to a natural scale-separation, the so-called Zeman wavenumber

* priyanka.maity@icts.res.in

† rama@icts.res.in

‡ samriddhisankarray@gmail.com

N	δt	ν	α	N_p	ϵ	η	τ_η	λ	Re_λ	$\tau_\eta/\delta t$	η/dx	$k_{\max}\eta$	Ω	Ro
512	4×10^{-4}	10^{-3}	5×10^{-3}	10^6	0.89	6×10^{-3}	3.33×10^{-2}	0.12	90	86	0.6	2.56	$0 - 2.0$	$\infty - 0.06$

TABLE I. Parameters for the simulations in a 2π periodic cube: N is number of collocation points in each direction, δt is the time step of integration, ν is the kinematic viscosity of the fluid, α is the coefficient of the large scale friction, and N_p represent the number of tracer particles seeded in the flow. The mean energy dissipation rate $\epsilon = 2\nu \sum_k k^2 E(k)$, while $\eta = \left(\frac{\nu^3}{\epsilon}\right)^{1/4}$ and $\tau_\eta = \left(\frac{\nu}{\epsilon}\right)^{1/2}$ are the Kolmogorov length and time scales, respectively. The Taylor length scale of the flow is denoted by $\lambda = \sqrt{\frac{15\nu^2_{\text{rms}}}{\epsilon}}$ (where, u_{rms} is the root-mean-squared fluid velocity) and $Re_\lambda = u_{\text{rms}}\lambda/\nu$ represents the Reynolds number corresponding to the Taylor microscale. The number of collocation points determine the grid spacing $dx = 2\pi/N$ and the maximum wave number k_{\max} of the simulations. The rotation rate Ω defines the Rossby number $Ro = \frac{u_{\text{rms}}}{2L\Omega}$. We choose seven different strengths of rotation rates $\Omega = 0, 0.1, 0.5, 0.75, 1.0$, and 2.0 yielding Rossby numbers $Ro = \infty, 1.23, 0.24, 0.16, 0.12, 0.08$, and 0.06 , respectively.

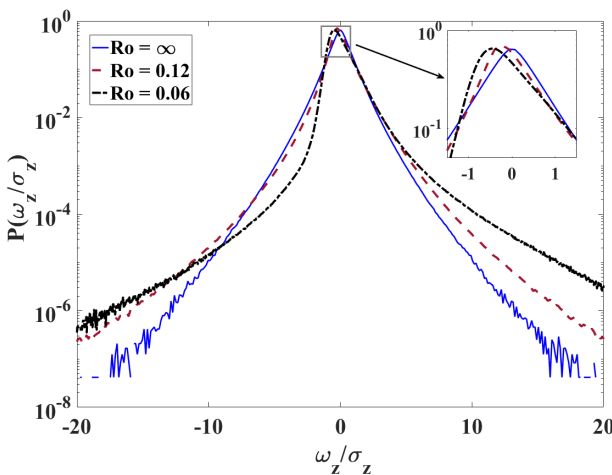


FIG. 1. Probability distribution functions of the vertical component of the vorticity ω_z , normalized by its standard deviation σ_z for $Ro = \infty$ (blue solid curve), 0.12 (red dashed curve), and 0.06 (black dashed-dotted curve)

ber $k_\Omega \sim \sqrt{\frac{\Omega^3}{\epsilon}}$, which sets the scale where the local fluid turnover time ($\epsilon^{-1/3}k^{-2/3}$) is of the same order as Ω^{-1} . For strongly rotating flows ($Ro \ll 1$) and wavenumbers $k < k_\Omega$, the kinetic energy spectrum $E(k) = |u_k|^2$ tends to steepen leading to a scaling $E(k) \sim k^{-2}$ [26, 31, 36–38] while retaining the usual Kolmogorov spectrum $E(k) \sim k^{-5/3}$ at higher wavenumbers.

We solve the Navier-Stokes equation in the rotating frame (Eq. 1) through the standard pseudo-spectral method [39], with a second-order Adams-Bashforth scheme for time-marching, in a 2π -periodic cubic box with the axis of rotation being the z -axis. We use $N^3 = 512^3$ collocation points and an external constant energy injection force, acting on wavenumbers $k \leq 3$, to drive the system to a statistically steady state with a Taylor-scale Reynolds number $Re_\lambda \approx 100$. As is common in such numerical simulations, we introduce a small additional frictional term in the form of an inverse Laplacian, with a small coefficient $\alpha = 0.005$ to damp out the energy which piles up at the smaller modes due to the inverse cascade set in motion by the rotation. The details of the simulation are presented in Table I.

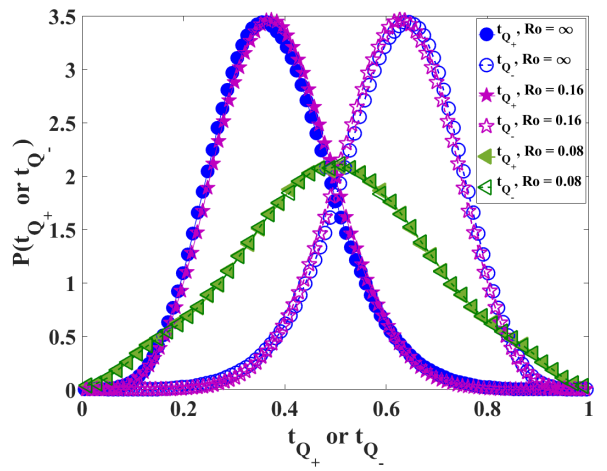


FIG. 2. Probability distribution functions of the fraction of time particles spend in vortical (t_{Q_+}) (filled markers) and straining (t_{Q_-}) (open markers) regions for $Ro = \infty$ (circles), 0.16 (stars), and 0.08 (triangles).

We begin by addressing the question of how the reorganization of the flow, in the presence of a Coriolis force, influences the trajectories of tracers, which sample the phase space of the flow uniformly. We therefore seed, randomly and homogeneously, our flow, once it has reached a statistically stationary state, with $N_p = 10^6$ tracer particles with initial velocities identical to the velocity of the fluid at particle position. The dynamics of a single tracer, with a trajectory \mathbf{r}_p , is given by:

$$\frac{d\mathbf{r}_p}{dt} = \mathbf{v}_p; \quad \mathbf{v}_p = \mathbf{u}(\mathbf{r}_p). \quad (2)$$

Numerically, we use a trilinear interpolation scheme to obtain the fluid velocity $\mathbf{u}(\mathbf{r}_p)$ at particles positions, since these are typically off-grid.

For such steady states in the presence of rotation, as the Rossby number decreases, the emergence of strong coherent cyclonic vortices—due to enhanced stretching of cyclonic vortices and destabilization of anti-cyclonic vortices—leads to an increased positive skewness in the probability distribution function (pdf) of the vorticity component ω_z in the direction z of the axis of rotation. In Fig. 1 we show this distribution function, measured along the Lagrangian trajectories of the

particles, for different values of Ro . Our observation, that the pdf becomes increasing skewed, is consistent with that seen in experiments of rotating flows, such as by Morize, *et al.* [21]. Furthermore, these distributions show an exponential tail and peak (Fig. 1, inset) at mildly negative values of ω_z (with decreasing Ro) ensuring an overall positive skewness for $Ro \ll 1$.

A convenient way to measure the correlation between the structure—broadly vortical and straining—of the flow and the Lagrangian dynamics is through the second invariant of the velocity gradient tensor $\nabla \mathbf{u}$ [40, 41]:

$$Q = \frac{1}{2}(\|\Theta\|^2 - \|\Sigma\|^2), \quad (3)$$

where $\|\Theta\| = \text{Tr}[\Theta\Theta^T]^{1/2}$ and $\|\Sigma\| = \text{Tr}[\Sigma\Sigma^T]^{1/2}$; the superscript T denotes the transpose of a matrix and Tr its trace. The symmetric component of the velocity gradient tensor, or the rate-of-strain tensor, is given by $\Sigma = \frac{1}{2}[\nabla \mathbf{u} + (\nabla \mathbf{u})^T]$ and the anti-symmetric component by $\Theta = \frac{1}{2}[\nabla \mathbf{u} - (\nabla \mathbf{u})^T]$. Hence, Q gives a local measure of the relative strengths of these two tensors. (Note that the non-standard notation Θ and Σ are used because the symbols Ω and S are taken up for the mean rotation rate of the system and the symmetry function, respectively.) Such a local measurement of Q is thus a useful diagnostic to determine if the flow at any point, in an Eulerian framework, is dominated by vortices ($Q \geq 0$) or by straining regions ($Q < 0$). Similarly this ‘ Q ’ criterion can be applied in Lagrangian measurements, such as ours, by measuring the Q value of the flow seen by a Lagrangian particle along its trajectory.

With this formalism, we begin by investigating how the emergence of coherent columnar vortices, with decreasing Rossby numbers, leads to a bias in the Lagrangian sampling of the flow, and hence to the flight-crash picture. We begin by calculating the fraction of time spent by the tracers in vortical t_{Q+} and straining t_{Q-} regions. This is done most conveniently by measuring Q along each tracer trajectory which allows us to calculate, for each trajectory, the fraction of time it has spent in vortical t_{Q+} ($Q \geq 0$) or straining t_{Q-} ($Q < 0$) regions; from the data of these times for N_p , we are able to construct the pdf of these residence times. In Fig. 2 we show the distribution of these times for different Rossby numbers (including the case of no rotation). We find that for weak ($Ro = 0.16$) or no ($Ro = \infty$) rotation, Lagrangian particles spend a disproportionately large fraction of time in strain-dominated regions as compared to vorticity dominated ones (as seen by the blue and magenta curves in Fig 2). This is because for no (or weak) rotation, the flow is characterized by weaker but spatially extended straining regions in contrast to the more localised and sparse regions of strong vorticity. Hence the tracers spend more time in straining regions than in vortical ones. As $Ro \rightarrow 0$, the flow re-organizes itself with a proliferation of extended vortical structures. Consequently, the fraction of the flow with positive Q becomes comparable to that with negative Q and tracers spend more time in vortical regions than they would be if the effect of rotation is weak. In fact, for $Ro = 0.08$ it can be seen (green curves in Fig 2) that the distribution of t_{Q+} and t_{Q-} are now practically identical.

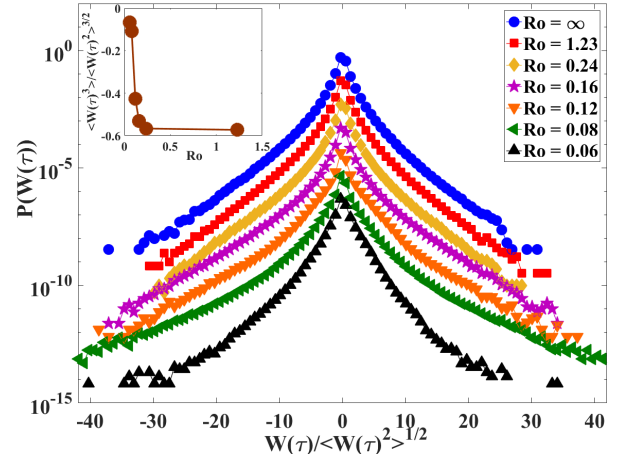


FIG. 3. Probability distribution function of the energy increment $W(\tau) = E(t+\tau) - E(t)$, normalised by its root-mean-square value $\langle W(\tau)^2 \rangle^{1/2}$ for $\tau/\tau_\eta = 2$. The curves are for different values of Ro (see legend) and artificially shifted by factors of 10 for clarity. (Inset) The skewness of the pdfs of $W(\tau)$ as a function of Ro .

It is important to recall that Bhatnagar, *et al.*, [42] showed an apparently contrary behaviour for their Lagrangian measurements in a non-rotating flow. This is due to their use of the Δ -criterion [43] which over-samples the vortices by considering regions which have *small* negative values of Q . We have checked that our results are consistent with Bhatnagar, *et al.*, [42] when we use the Δ -criterion and not the Q -criterion.

This striking feature of the residence times of tracers in different regions of the flow, as a function of the Rossby number, leads us to ask if it plays a role in negating flight-crashes as a useful probe for irreversibility. We begin by measuring the probability distribution function of the Lagrangian energy increments $W(\tau) = E(t+\tau) - E(t)$, where $E(t)$ is the kinetic energy of the tracer at any time t . In non-rotating flows [1, 2], this distribution is negatively skewed because gains $W(\tau) > 0$ in energy are slower than their dips $W(\tau) < 0$ for any fixed τ . In Fig. 3, we plot this distribution, along with the skewness (see inset) as a function of Ro , at time $\tau/\tau_\eta = 2.0$, for several different values of the Rossby number (artificially separated for clarity). We see, and quantify through the inset in Fig. 3, a less skewed behaviour of the energy increments as $Ro \rightarrow 0$. (It should be noted that the choice of $\tau/\tau_\eta = 2.0$ is arbitrary; the pdfs of the energy increments are always negatively skewed but this is more pronounced when the time-increments are small.)

A natural interpretation of such distributions are made in the light of fluctuation-dissipation theorems which, at least for simpler systems which can be modelled as being coupled to thermostats, states that [44]

$$S \equiv \ln \left[\frac{P(-W)}{P(W)} \right] \propto W, \quad (4)$$

where S , as seen, is a symmetry function constructed from the ratio of energy jump probabilities. Xu, *et al.* [1], found their measurements to be strongly fluctuating and hence found no

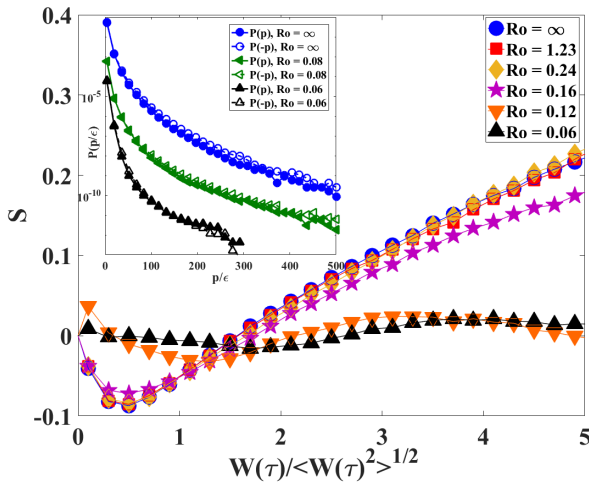


FIG. 4. Representative plots of the symmetry function S versus the energy increment $W(\tau)$ normalized by its root-mean-square value $\langle W(\tau)^2 \rangle^{1/2}$ for $\tau/\tau_\eta = 2$ for different values of Ro (see legend). Inset: Probability distribution functions of the negative (open symbols) and positive (filled symbols) values of the Lagrangian power for $Ro = \infty, 0.08$, and 0.06 ; the negative tail has been reflected for ease of comparison.

convincing evidence that such a function S actually scales linearly with W . However, in our simulations, shown in Fig. 4), given the volume of data and statistics, a plot of the symmetry function S versus the normalized W shows a much cleaner trend. We see a small window of nearly-linear behavior at moderate values of $W(\tau)$ for cases of no or negligible rotation. On the other hand, when the Rossby number is very small, the plot of S is essentially flat and lies close to 0. This, then, is the first clear evidence that the skewness in the distribution of W diminishes as the flow reorganizes itself under strong rotation. Thus a combination of emergent coherent vortices and inverse cascade in strongly rotating flows—while remaining dissipative—seems to negate the possibility of flight-crash events along Lagrangian trajectories as a probe for measuring the irreversibility of the flow. This conclusion is further strengthened in the inset of Fig. 4 where we plot the (suitably normalized) distributions of the positive and negative values of the power $p \equiv dE/dt$ for different values of the Rossby number. For no or negligible rotations, it is visible that at higher power, the curve for negative power lies above that for positive power (reflective of the irreversibility and flight-crashes [1]); however when $Ro \ll 1$, the two pdfs are hardly distinguishable.

Since the macroscopic dissipation is held constant in our calculations, this lack of flight-crashes must stem from the emergent anisotropic geometry of the flow under rotation. To quantify this, we measure the power p as a function of time for our N_p Lagrangian trajectories from which it is possible to construct the fraction of time that a particle spends in gaining ($p > 0$) or losing ($p < 0$) energy. For homogeneous, isotropic turbulence, the proliferation for flight-crash events would suggest that the fraction of time t_{gain} spent in gaining energy must be larger than the fraction of time t_{loss} spent in

losing it. In Fig. 5(a) we plot the distribution of both t_{gain} and t_{loss} to find evidence for this: The (Gaussian) distribution of the time for energy gain is shifted to the right compared to the one for energy loss. However, as rotation starts to dominate, the distribution for both start becoming identical with a mean fraction of time spent for either gaining or losing energy being half (Figs. 5 (b) and (c)). This variation of the pdfs of t_{gain} and t_{loss} follow a trend similar to, but not exactly, as the distributions of the residence times in Fig. 2. This is because the collapse of pdfs of t_{Q+} and t_{Q-} onto each other, as $Ro \rightarrow 0$, is much more dramatic when compared to the gradual merging of the pdfs of t_{gain} and t_{loss} for similar changes in Ro . This is expected, of course, because unlike a direct measurement of the residence times, the fraction of times spent in losing or gaining kinetic energy, although correlated to where it resides in the flow, is not uniquely determined by the local flow geometry.

We also measure the distribution of p along Lagrangian trajectories *and* conditioned on whether they are in vortical ($Q \geq 0$) or in straining ($Q < 0$) regions. In Fig. 6 we plot the pdf of the power, conditioned on the geometry of the flow for $Ro = 0.16$, and see evidence that in straining regions, energy gains are more probable than energy losses, whereas in vortical regions the probabilities are similar. Now, as rotation is increased, the fraction of the flow in vortical regions is higher. Moreover these vortices are stronger and more coherent on an average. This can be seen in the Lagrangian skewness in the distribution of Q (Fig. 6, inset). Therefore at higher rotation rates, gains in energy are as frequent, and have the same distribution, as losses.

What does all of this mean for the central question of this work, namely Lagrangian irreversibility and its connections with the geometry of the flow? In statistically steady state, Lagrangian reversibility or time reversibility should imply that the probability of energy gain ($p > 0$) or energy loss ($p < 0$) should be equal. Therefore, any asymmetry in the pdfs of p would suggest the breaking of Lagrangian or time reversibility in the system. One way to measure this irreversibility, is to consider the quantity [1]:

$$Ir = \frac{-\langle p^3 \rangle}{\epsilon^3}. \quad (5)$$

For homogeneous and isotropic turbulence, $Ir \gg 1$ and increases with the Reynolds number of the flow. This stems from the fact that “flight-crashes” proliferate in such flows with increasing Reynolds numbers leading to an ever-increasing skewness in the distribution of the power p . We have, however, seen that because of the Coriolis force, the flow reorganizes leading to, e.g., a depletion in the skewness of Q along Lagrangian trajectories. Could the effect be as strong in measurements of Ir ? In Fig. 7 we plot Ir as a function of Ro and find a sharp decrease as soon as $Ro < 1$. Indeed for $Ro \ll 1$, the decrease in the irreversibility is by an order of magnitude compared to the case where the rotation is negligible. (We have checked that our value of Ir for $\Omega = 0$ is consistent with the findings in Ref. [1].)

Indeed, in recent times, this issue of reversibility has been re-examined in a variety of problems which range from the

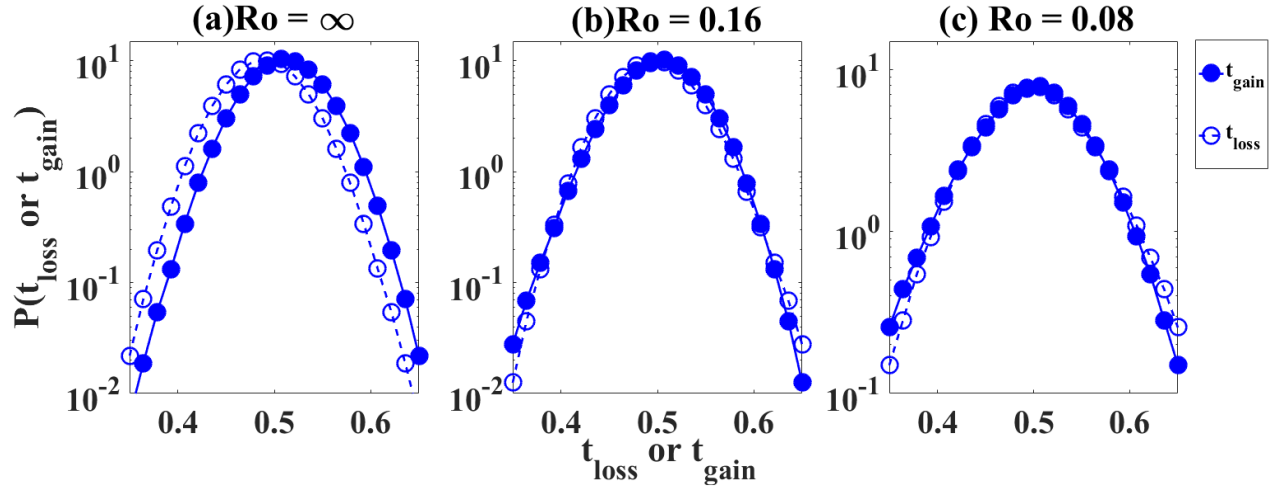


FIG. 5. Probability distribution functions of the fraction of time during which tracers gain t_{gain} (filled circles) and lose t_{loss} (open circles) for (a) $\text{Ro} = \infty$, (b) $\text{Ro} = 0.16$, and (c) $\text{Ro} = 0.08$.

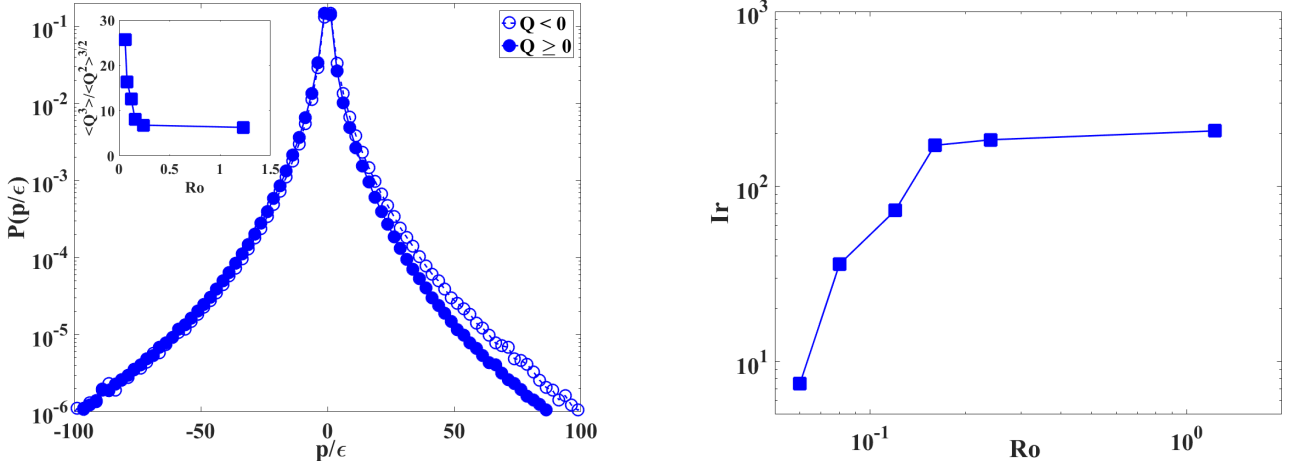


FIG. 6. Representative plots, for $\text{Ro} = 0.16$, of the pdf of the Lagrangian power, normalized by energy dissipation rate ϵ , conditioned on whether the particles are in vortical $Q \geq 0$ (filled circles) or straining regions $Q < 0$ (open circles). (Inset) The skewness of the Q showing a sharp increase with decreasing Rossby number.

use of the time-reversible Navier-Stokes equation [45] to how the suppression of small-scale intermittency through Fourier-decimation [46, 47] lead to an emergent reversibility when measure via Lagrangian Lyapunov exponents [48]. Our study is however different from these. Unlike the use of a fluctuating thermostat to replace the usual viscosity in the Navier-Stokes equation leading to time-reversibility or the suppression of a subset of triadic interactions to solve the equations on a quenched, disordered lattice, we show that even for the *true* equations of motion, rotation and the consequent emergence of coherent, anisotropic structures is enough to alter the statistics of Lagrangian trajectories. In particular, at high rotation rates, the notion of flights and crashes cease to exist and thus

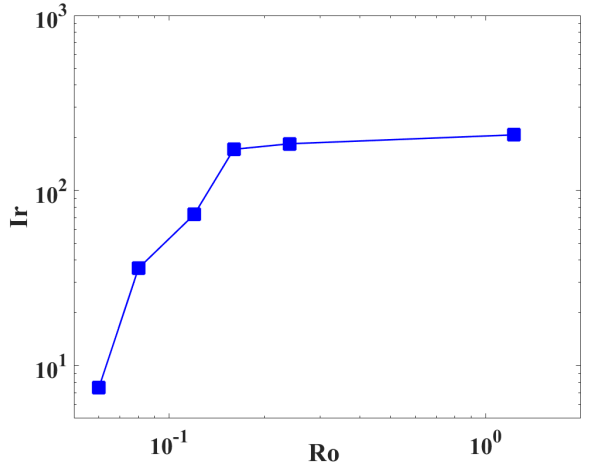


FIG. 7. The irreversibility Ir as a function of Ro showing a sharp increase, by an order of magnitude, as $\text{Ro} \rightarrow 1$.

does not allow an easy interpretation of time-irreversibility in terms of such Lagrangian probes. We hope that this work, which does not rely on modifications to the equations of hydrodynamics, will lead to experiments designed to look at this specific aspect of Lagrangian irreversibility in experiments in future.

We thank J. R. Picardo for useful suggestions and discussions and H. J. H. Clercx for several useful references. A part of this work was facilitated by a program organized at ICTS: *Turbulence from Angstroms to Light Years* (ICTS/Progitaly2018/01). The simulations were performed on the ICTS clusters *Mowgli*, *Tetris* and *Mario* as well as the work stations from the project ECR/2015/000361: *Goopy* and *Bagha*. SSR acknowledges DST (India) project ECR/2015/000361 for financial support.

-
- [1] H. Xu, A. Pumir, G. Falkovich, E. Bodenschatz, M. Shats, H. Xia, N. Francois, and G. Boffetta, Proc. Natl. Acad. Sci. (U.S.A) **111**, 7558 (2014).
- [2] A. Bhatnagar, A. Gupta, D. Mitra, and R. Pandit, Phys. Rev. E **97**, 033102 (2018).
- [3] H. P. Greenspan, *The Theory of Rotating Fluids.* (Cambridge Universiy Press, 1968).
- [4] H. K. Moffatt, Rep. Prog. Phys. **46**, 621 (1983).
- [5] P. Davidson, *Turbulence in Rotating , Stratified and Electrically Conducting Fluids.* (Cambridge University Press, 2013).
- [6] S. A. Barnes, Astrophys. J. **561**, 1095 (2001).
- [7] J. Y.-K. Cho, K. Menou, B. M. S. Hansen, and S. Seager, Astrophysic. J. **675**, 817 (2008).
- [8] T. Le Reun, B. Favier, A. J. Barker, and M. Le Bars, Phys. Rev. Lett. **119**, 034502 (2017).
- [9] J. Aurnou, M. Calkins, J. Cheng, K. Julien, E. King, D. Nieves, K. Soderlund, and S. Stellmach, Phys. Earth Planet In. **246**, 52 (2015).
- [10] H. Dumitrescu and V. Cardos, AIAA Journal **42**, 408 (2004).
- [11] L. M. Smith and F. Waleffe, Phys. Fluids **11**, 1608 (1999).
- [12] W.-C. Müller and M. Thiele, Europhys. Lett.) **77**, 34003 (2007).
- [13] P. D. Mininni, A. Alexakis, and A. Pouquet, Phys. Fluids **21**, 015108 (2009).
- [14] P. Bartello, J. Atmos. Sci. **52**, 4410 (1995).
- [15] O. Métais, P. Bartello, E. Garnier, J. Riley, and M. Lesieur, Dynam. Atmos. Oceans **23**, 193 (1996).
- [16] E. Yarom, Y. Vardi, and E. Sharon, Phys. Fluids. **25**, 085105 (2013).
- [17] G. P. Bewley, D. P. Lathrop, L. R. M. Maas, and K. R. Sreenivasan, Phys. Fluids **19**, 071701 (2007).
- [18] E. Yarom, A. Salhov, and E. Sharon, Phys. Rev. Fluids **2**, 122601 (2017).
- [19] A. Ibbetson and D. J. Tritton, J.Fluid Mech. **68**, 639672 (1975).
- [20] E. J. Hopfinger, F. K. Browand, and Y. Gagne, J. Fluid. Mech. **125**, 505534 (1982).
- [21] C. Morize, F. Moisy, and M. Rabaud, Phys. Fluids **17**, 095105 (2005).
- [22] F. Moisy, C. Morize, M. Rabaud, and J. Sommeria, J. Fluid Mech. **666**, 535 (2011).
- [23] P. Bartello, O. Métais, and M. Lesieur, J. Fluid. Mech. **273**, 129 (1994).
- [24] F. S. Godeferd and L. Lollini, J. Fluid Mech. **393**, 257308 (1999).
- [25] O. Zeman, Phys. Fluids **6**, 3221 (1994).
- [26] Y. Hattori, R. Rubinstein, and A. Ishizawa, Phys. Rev. E **70**, 046311 (2004).
- [27] B. Sreenivasan and P. A. Davidson, Phys. Fluids **20**, 085104 (2008).
- [28] A. Pouquet and P. D. Mininni, Philos. Trans. R. Soc. Lond., A **368**, 1635 (2010).
- [29] J. Proudman and H. Lamb, Proc. R. Soc. London, Ser. A **92**, 408 (1916).
- [30] G. I. Taylor and H. Lamb, Proc. R. Soc. of London, Ser. A **93**, 99 (1917).
- [31] L. Biferale, F. Bonaccorso, I. M. Mazzitelli, M. A. T. van Hinsberg, A. S. Lanotte, S. Musacchio, P. Perlekar, and F. Toschi, Phys. Rev. X **6**, 041036 (2016).
- [32] B. Gallet, A. Campagne, P.-P. Cortet, and F. Moisy, Phys. Fluids **26**, 035108 (2014).
- [33] L. D. Castello and H. J. H. Clercx, J. Phys.: Conf. Ser. **318**, 052028 (2011).
- [34] L. Del Castello and H. J. H. Clercx, Phys. Rev. Lett. **107**, 214502 (2011).
- [35] L. Del Castello and H. J. H. Clercx, Phys. Rev. E **83**, 056316 (2011).
- [36] Y. Zhou, Phys. Fluids **7**, 2092 (1995).
- [37] C. N. Baroud, B. B. Plapp, Z.-S. She, and H. L. Swinney, Phys. Rev. Lett. **88**, 114501 (2002).
- [38] P. K. Yeung and Y. Zhou, Phys. Fluids **10**, 2895 (1998).
- [39] C. Canuto, M. Y. Hussaini, A. Quarteroni, and T. A. Zang, *Spectral Methods in Fluid Dynamics*, 1st ed., Scientific computation (Springer, 2011).
- [40] J. C. R. Hunt, A. A. Wray, and P. Moin, in *Studying Turbulence Using Numerical Simulation Databases.* 2 (1988).
- [41] J. Jeong and F. Hussain, J. Fluid Mech. **285**, 6994 (1995).
- [42] A. Bhatnagar, A. Gupta, D. Mitra, R. Pandit, and P. Perlekar, Phys. Rev. E **94**, 053119 (2016).
- [43] M. S. Chong, A. E. Perry, and B. J. Cantwell, Phys. Fluid. A **2**, 765 (1990).
- [44] S. Ciliberto, S. Joubaud, and A. Petrosyan, J. Stat. Mech. **2010**, P12003 (2010).
- [45] V. Shukla, B. Dubrulle, S. Nazarenko, G. Krstulovic, and S. Thalabard, ArXiv e-prints (2018), arXiv:1811.11503.
- [46] U. Frisch, A. Pomyalov, I. Procaccia, and S. S. Ray, Phys. Rev. Lett. **108**, 074501 (2012).
- [47] S. S. Ray, Pramana **84**, 395 (2015).
- [48] S. S. Ray, Phys. Rev. Fluids **3**, 072601 (2018).